

NIR - responsive nano - holed titanium alloys surfaces: a photothermally activated antimicrobial biointerface

Denise B. Pistonesi ^[a, §], Federico Belén ^[a, §], Juan M. Ruso ^[b], M. Eugenia Centurión ^[a],
M. Gabriela Sica ^[c, d], Marcelo F. Pistonesi ^[a], and Paula V. Messina ^{[a]*}

[a] Department of Chemistry, Universidad Nacional del Sur, INQUISUR – CONICET, B8000CPB, Bahía Blanca, Argentina. [b] Soft Matter and Molecular Biophysics Group, Department of Applied Physics and iMATUS, University of Santiago de Compostela, 15782 Santiago de Compostela, Spain. [c] Department of Biology, Biochemistry and Pharmacy, Universidad Nacional del Sur, B8000CPB, Bahía Blanca, Argentina. [d] Department of Health Sciences, Universidad Nacional del Sur, B8000CPB, Bahía Blanca, Argentina.

(*) Author to whom correspondence should be addressed. Tel: +54 291 4595159. Fax: +54 291 4595160. Electronic mail: pmessina@uns.edu.ar.

(§) Denise B. Pistonesi and Federico Belén contributed equally to this work.

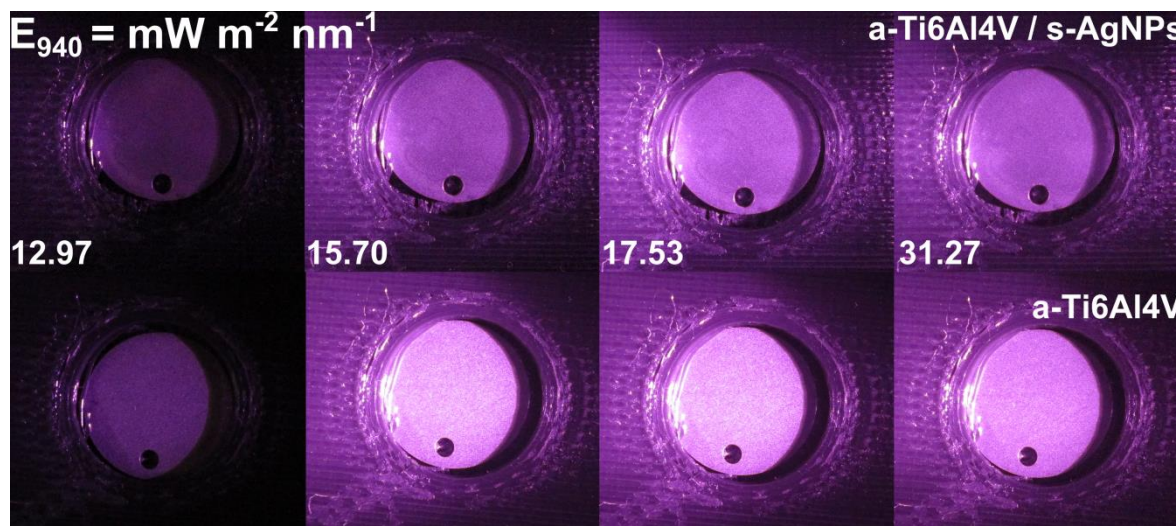


Figure 1ESI. Anodized Ti6Al4V discs immersed in sphere-like AgNPs reaction medium throughout 7h used as a second control (*a*-Ti6Al4V / *s*-AgNPs) compared to *a*-Ti6Al4V.

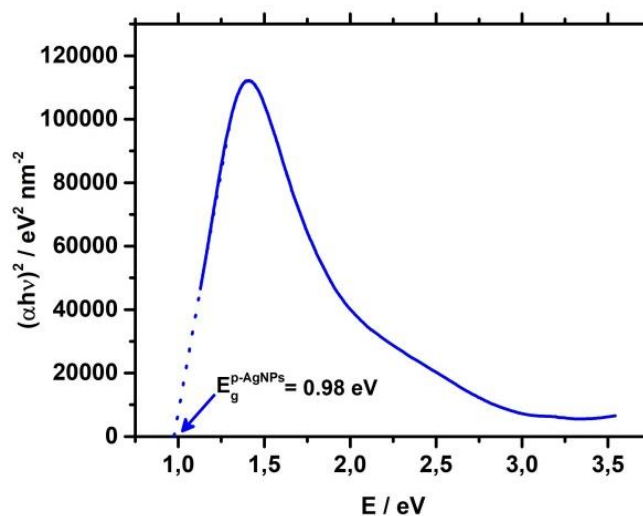


Figure 2ESI. Absorption coefficient, α , was used to analyze the absorption edge for direct transitions in *p*-AgNPs. α was computed as indicated Hassan et al. ¹

The shape and size of the nano-holed structure were interpreted in terms of their Feret's diameter (D_F), Feret's angle (F_{ang}), roundness (R) and circularity (C). Originally, *a*-Ti6Al4V, exhibits a uniform and regular distribution pattern along macro- and nano- scale levels. The oxide layer presents a homogeneous network of interconnected nano-pores, with a center-to-center distance of about 35.5 ± 2.2 nm, TiO_2 inter-void barriers of about 7.2 ± 0.6 nm in their upper and of 22.0 ± 1.2 nm in their basal diameter. Titania cavities have,

28.5 ± 2.1 nm on their upper portion and 15.2 ± 0.9 nm in their basal distance, given rise to the ratio between spacing and basal diameter of ≈ 1.88 .²

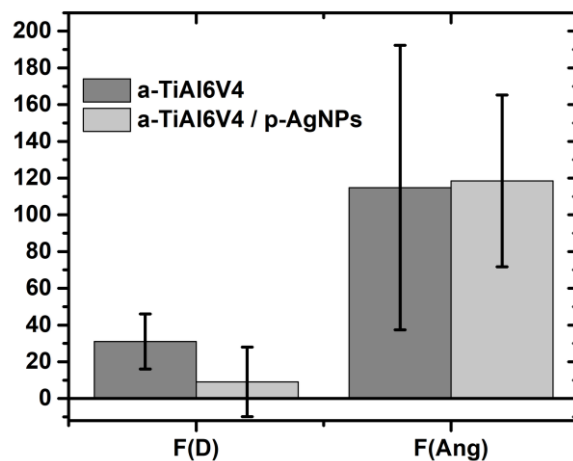


Figure 3ESI. Feret's diameter (D_F) and Feret's angle (F_{ang}) of original anodized Ti6Al4V sheets and of a-Ti6Al4V / p-Ag-NPs surfaces after immersion throughout 7 h in prism-shaped nanosilver reaction media.

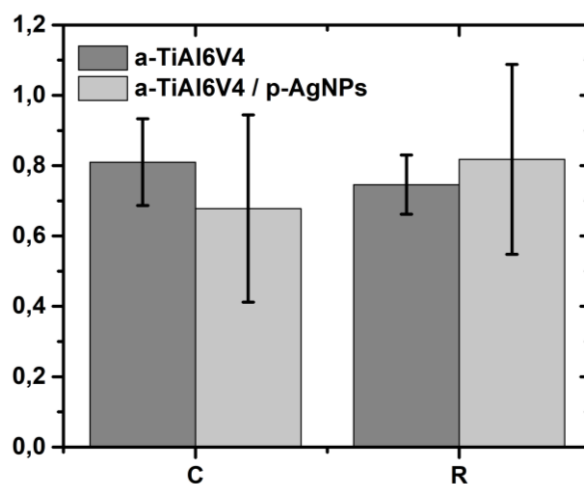


Figure 4ESI. Roundness (R) and circularity (C) of original anodized Ti6Al4V sheets and of a-Ti6Al4V / p-Ag-NPs surfaces after immersion throughout 7 h in prism-shaped nanosilver reaction media.

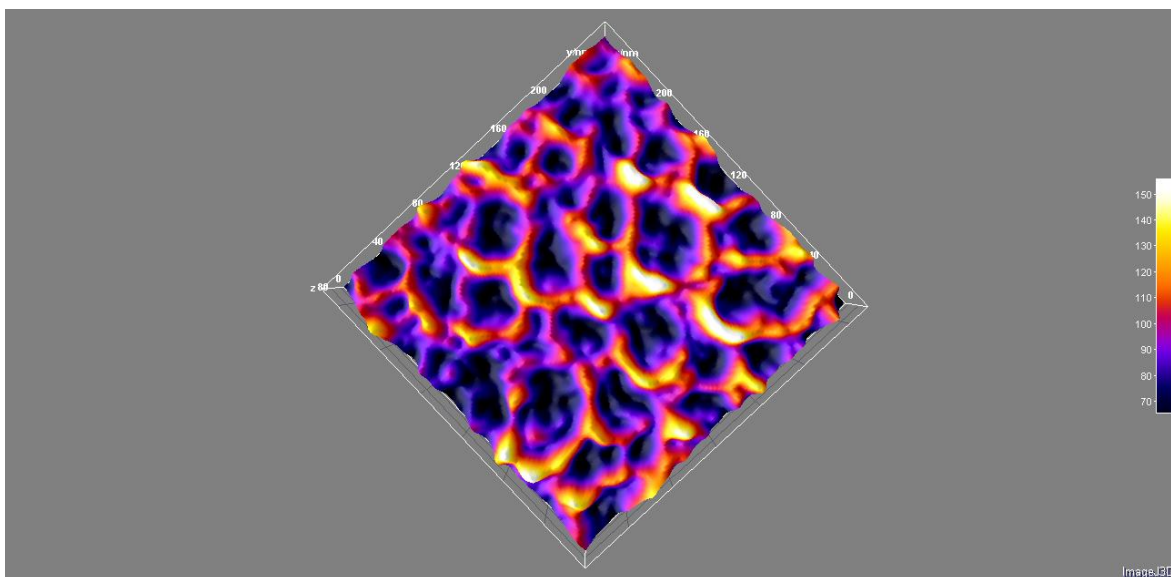


Figure 5ESI. 3D surface plot of a-Ti6Al4V / p-Ag-NPs substrate displaying the packing array of nano-holes after immersion throughout 7 h in prism-shaped nanosilver reaction media.

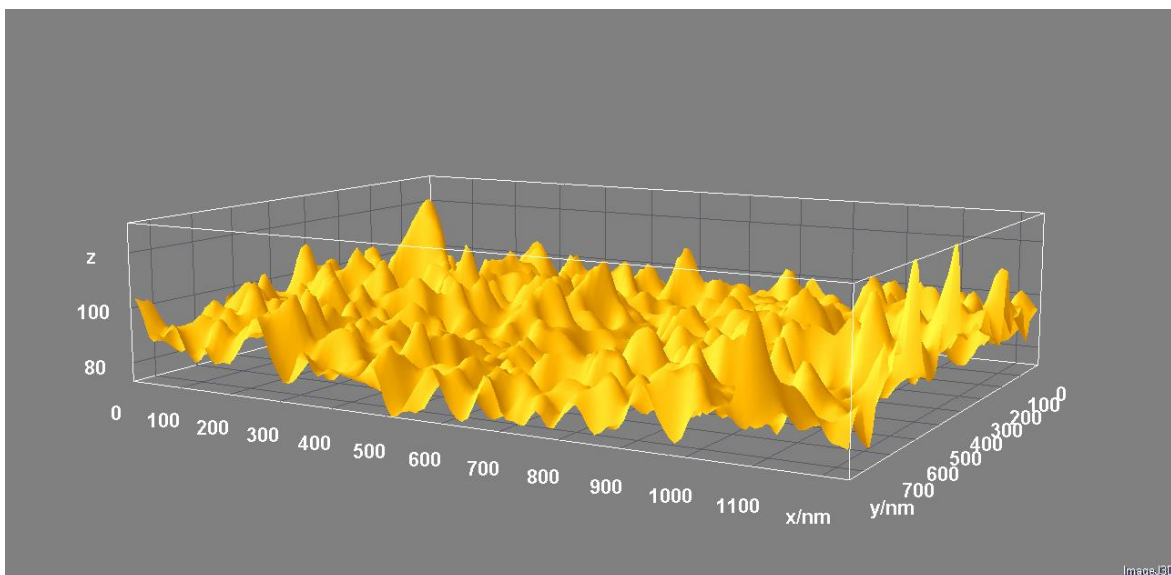


Figure 6ESI. Inverted colored 3D surface plot constructed from HR-SEM microphotograph of a-Ti6Al4V / p-Ag-NPs sheet after immersion throughout 7 h in prism-shaped nanosilver reaction media.

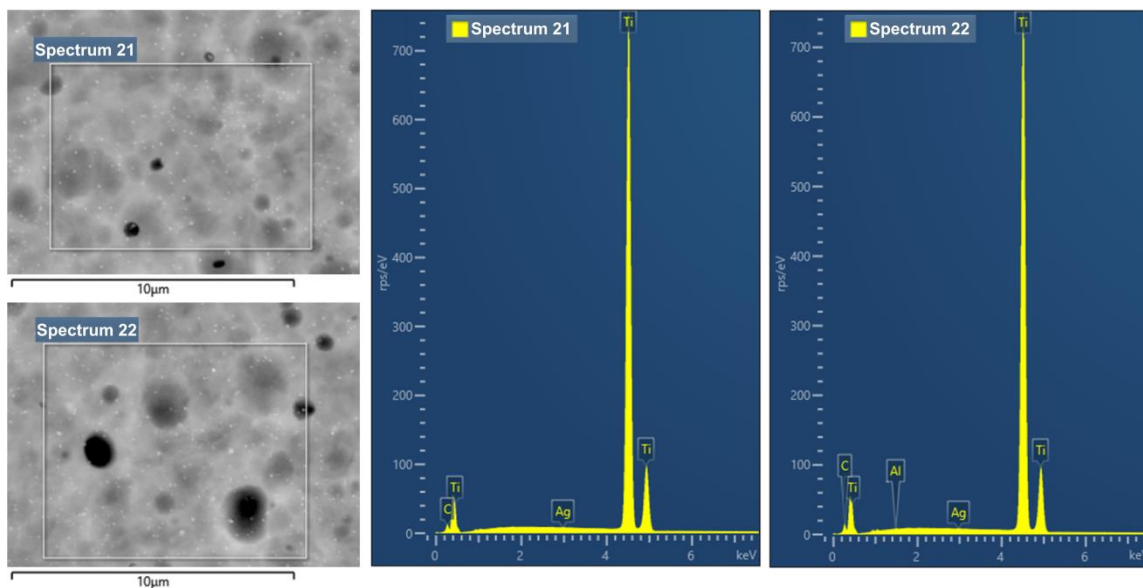


Figure 7ESI. EDX microanalysis of *a*-Ti6Al4V / *p*-Ag-NPs. (Spectrum 21) as obtained follows *in situ* generation procedure (7h) and (Spectrum 22) after their immersion in Milli Q water throughout 24 h.

Wt.%	C	Ti	Al	Ag	
Spectrum 21	2.16	96.91		0.93	100.00
Spectrum 22	2.55	96.46	0.04	0.95	100.00

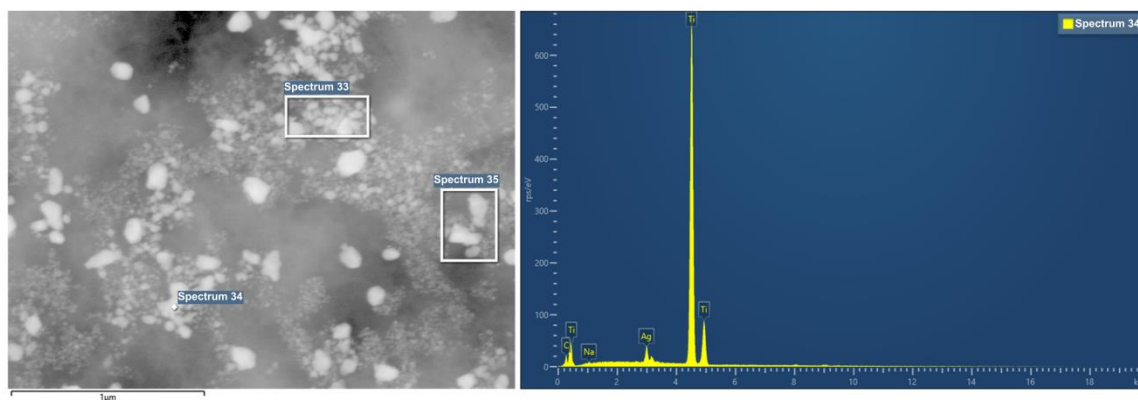


Figure 8ESI. EDX microanalysis of *p*-Ag-NPs clusters.

Wt.%	C	Na	Ti	Ag	
Spectrum 33	3.97	0.34	92.81	2.88	100.00
Spectrum 34	3.36	0.34	92.07	4.23	100.00
Spectrum 35	3.29	0.28	94.95	1.48	100.00

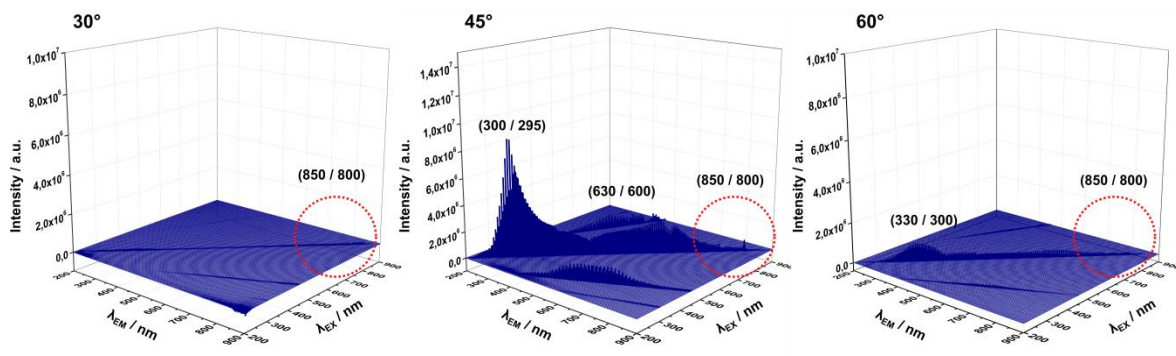


Figure 9ESI. 3D PL patterns recorded at 30, 45 and 60° of incident radiation Ti6Al4V / s-AgNPs surfaces. Bands indicated were expressed as ($\lambda_{EM} / \lambda_{EX}$). Missing band at (850 / 800) was indicated in the red circle.

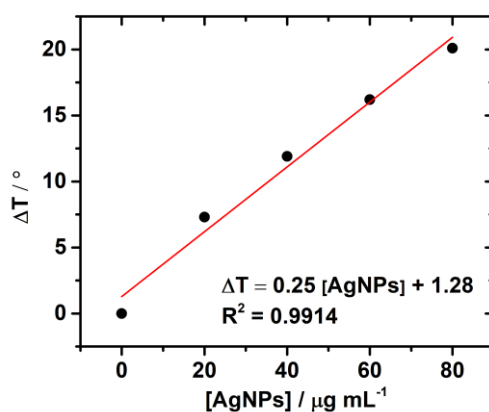


Figure 10ESI. Temperature increase after NIR plasmonic stimulation of different concentration prism-shaped AgNPs' dispersion. $t = 600$ seconds of NIR laser irradiation at 904 nm ($E = 83.6 \text{ mW cm}^{-2}$)

Table 1ESI. Photothermal conversion efficiency, η , of prism-shaped AgNPs' dispersions (p -AgNPs) and α -Ti6Al4V / p -AgNPs surfaces excited at 904 nm.

p - AgNPs	$T_{\max} / ^\circ\text{C}$	τ_S / s	hS / mW^{-1}	$T_{\max} - T_{\text{surr}} / ^\circ$	$Q_{\text{dis}} / \text{mW}$	$\eta / \%$
14 $\mu\text{g mL}^{-1}$	30.5	67.2 \pm 9.7	64 \pm 4.3	7.3 \pm 0.2	230.4 \pm 4.5	49.7
40 $\mu\text{g mL}^{-1}$	35.1	114.4 \pm 16.2	37 \pm 2.1	11.9 \pm 0.2	133.2 \pm 3.2	64.4
60 $\mu\text{g mL}^{-1}$	39.4	176.5 \pm 16.5	24 \pm 1.1	16.2 \pm 0.2	86.4 \pm 2.7	63.4
80 $\mu\text{g mL}^{-1}$	43.3	223.4 \pm 14.9	19 \pm 0.9	20.1 \pm 0.2	68.4 \pm 1.5	65.7
α -Ti6Al4V/ p -AgNPs	32.3	94.1 \pm 9.3	1.73	6.9 \pm 0.2	0.346	35.1

Table 2ESI. Minimum bactericidal concentration (MBC) and minimum inhibitory concentration (MIC) for the different synthesized Ag-NPs.

Ag-NPs	<i>Staphylococcus aureus</i> / CFU mL ⁻¹				
	10 ²	10 ³	10 ⁴	10 ⁵	10 ⁶
	MIC / $\mu\text{g mL}^{-1}$				
Spherical-shaped	25	25	25	25	50
Prism-shaped	3.1	3.1	3.1	6.5	50
	MBC / $\mu\text{g mL}^{-1}$				
Spherical-shaped	≥ 25	≥ 25	≥ 25	≥ 25	≥ 50
Prism-shaped	≥ 3.1	≥ 3.1	≥ 3.1	≥ 12.5	≥ 50

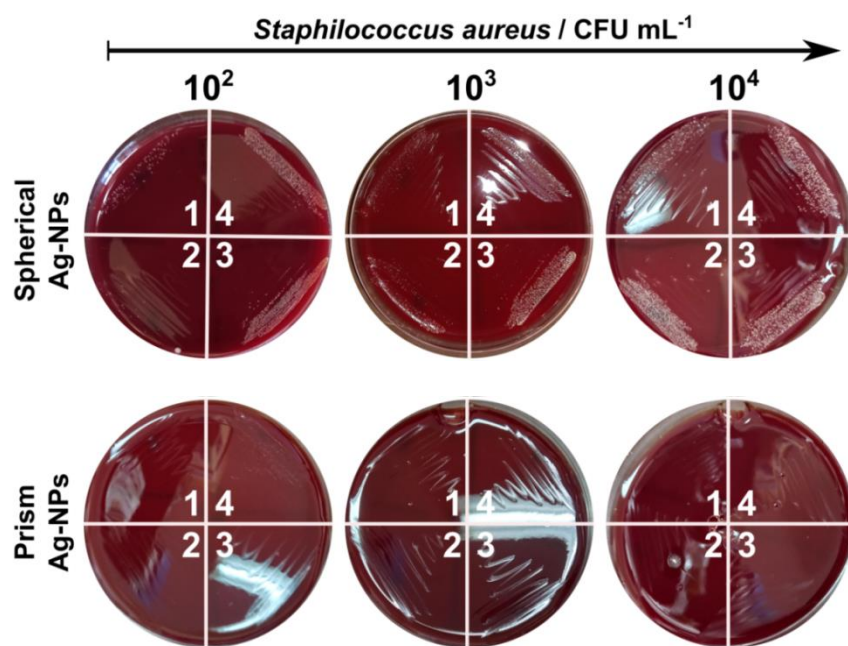


Figure 11ESI. AgNPs of different shape effect on *Staphylococcus aureus* viability. Representative images of *Staphylococcus aureus* colonies on blood agar platelets. *Staphylococcus aureus* with different bacteria concentrations ($10^2 - 10^4$ CFU mL⁻¹) were treated without spherical and prims-shaped Ag-NPS with different concentrations: (1) 25 $\mu\text{g mL}^{-1}$; (2) 12.5 $\mu\text{g mL}^{-1}$; (3) 6.2 $\mu\text{g mL}^{-1}$ and (4) 3.1 $\mu\text{g mL}^{-1}$

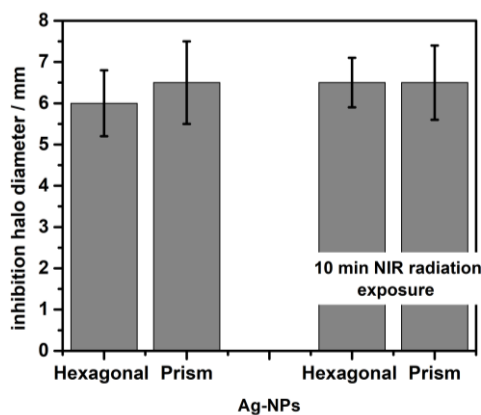


Figure 12ESI. Bacterial inhibition performed after exposing Ag-NPs to 10 minutes of NIR radiation. Statistical analysis was performed among different materials, $n = 4$, $*p < 0.05$; significant differences between the samples are indicated with brackets.

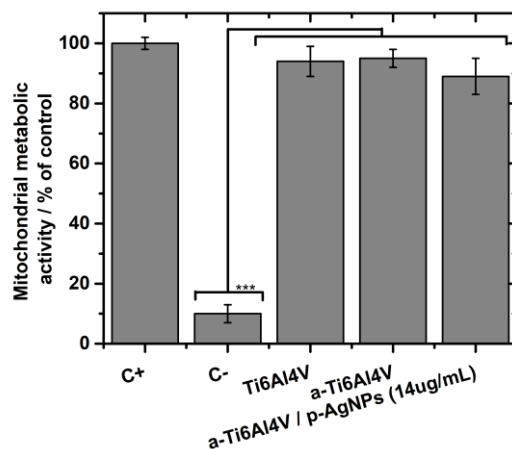


Figure 13ESI. Mitochondrial metabolic activity of preosteoblast MC3T3-E1 cells. Statistical analysis was performed among different materials, $n = 4$, $*p < 0.05$; significant differences between the samples are indicated with brackets. Wells containing cells but no substrates were used as positive control (C+) and wells containing a-Ti6Al4V/p-AgNPs substrates with medium but without cells were used as negative controls (C-). Mitochondrial metabolic activity (%) = $(OD_{570} / OD_{570, C+}) \times 100$.

References

1. N. Hassan, V. Verdinelli, J. M. Ruso and P. V. Messina, *Langmuir*, 2011, **27**, 8905-8912.
2. F. Belén, A. N. Gravina, M. F. Pistonesi, J. M. Ruso, N. A. García, F. D. Prado and P. V. Messina, *ACS Appl. Mater. Interfaces*, 2022, **14**, 5843-5855.